PCCP

Accepted Manuscript

This is an *Accepted Manuscript*, which has been through the Royal Society of Chemistry peer review process and has been accepted for publication.

Accepted Manuscripts are published online shortly after acceptance, before technical editing, formatting and proof reading. Using this free service, authors can make their results available to the community, in citable form, before we publish the edited article. We will replace this *Accepted Manuscript* with the edited and formatted *Advance Article* as soon as it is available.

You can find more information about *Accepted Manuscripts* in the **Information for Authors**.

Please note that technical editing may introduce minor changes to the text and/or graphics, which may alter content. The journal's standard **Terms & Conditions** and the **Ethical guidelines** still apply. In no event shall the Royal Society of Chemistry be held responsible for any errors or omissions in this *Accepted Manuscript* or any consequences arising from the use of any information it contains.

Journal Name

Excited-state dynamics of guanosine in aqueous solution revealed by time-resolved photoelectron spectroscopy: experiment and theory[†]

Franziska Buchner,[a] Berit Heggen,[b] Hans-Hermann Ritze,[a] Walter Thiel,[b] and Andrea Lübcke,[*a]

Time-resolved photoelectron spectroscopy is performed on aqueous guanosine solution to study its excited-state relaxation dynamics. Experimental results are complemented by surface hopping dynamic simulations and evaluation of the excited-state ionization energy by Koopmans' theorem. Two alternative models for the relaxation dynamics are discussed. The experimentally observed excited-state lifetime is about 2.5 ps if the molecule is excited at 266 nm and about 1.1 ps if the molecule is excited at 238 nm. The experimental probe photon energy dependence of the photoelectron kinetic energy distribution suggests that the probe step is not vertical and involves a doubly-excited autoionizing state.

1 Introduction

Although DNA bases strongly absorb UV light, they are astonishingly photostable, which is the basis for the photostability of DNA, itself. The key to this photostability is their ultrafast, radiationless excited-state decay, which involves non-adiabatic processes at conical intersections. This general picture is widely accepted, although the detailed relaxation processes of individual DNA bases are not yet fully resolved. The excited-state relaxation of guanine (Gua) or its derivatives has been investigated experimentally both in the gas phase and the solution phase. In the gas phase, photoelectron imaging[1] and photoionization[2,3] were used, while in the solution phase transient absorption[4] and fluorescence up-conversion[5,6] were the techniques of choice. With the recent development of time-resolved liquid jet photoelectron spectroscopy, a new technique is at hand for investigating the solution phase excited-state dynamics. We have recently applied this technique to study the excited-state dynamics of adenine and adenosine (Ade/Ado)[7] as well as thymine and thymidine (Thy/Thd)[8] and demonstrated the potential of this technique for investigation of the excited-state dynamics of solvated molecules. In the present work, we investigate the excited-state dynamics of guanosine (Guo), the nucleoside of Gua, by time-resolved liquid

jet photoelectron spectroscopy. The chemical structures of the relevant species are given in Figure 1.
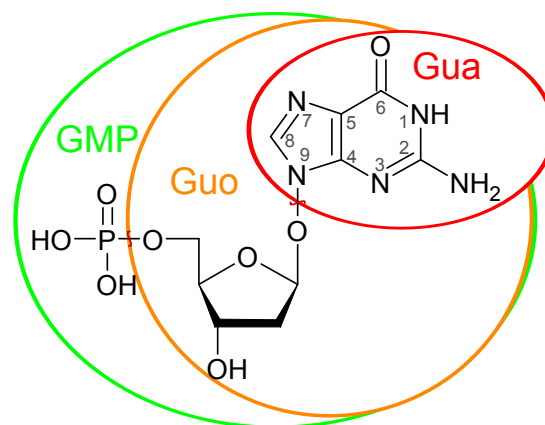
Fig. 1 Chemical structure of the DNA base guanine (Gua), its nucleoside guanosine (Guo), and its nucleotide guanosine monophosphate (GMP). In Gua and Guo, the missing groups are replaced by a hydrogen atom.

The optical absorption spectrum of Gua is dominated by two bright $\pi\pi^*$ transitions usually labeled as L_a and L_b. There are two dark states close to L_b in the gas phase, one of $n\pi^*$ character and one of $\pi\sigma^*$ character. There is quite large variation between different theoretical methods in describing how hydration affects the individual electronic states[9–11] and references therein. Altogether, one can say that L_a is stabilized under hydration, whereas

the $n\pi^*$ state is strongly destabilized. Most methods predict L_b to be only weakly affected by hydration.

Several theoretical studies explored the excited-state dynamics of Gua in the gas phase. All of these studies support the existence of a barrierless pathway connecting the Franck-Condon (FC) region and the conical intersection between S_1 and S_0. Several minimum energy structures were located at conical intersection seams for the gas phase at different levels of theory[12–15]. At the OM2/MRCI level, one conical intersection (CI_α) connecting the ground state with the first excited state is found at 3.52 eV and has an ^2E envelope puckered structure of the six-membered ring with the C2 atom being displaced out-of-plane (oop) and an increased C4-C5 bond length[15] (labelling of atoms according to Figure 1). A similar structure was found in ref.[14]. In the second S_0/S_1 CI, which is located at 2.8 eV at the OM2/MRCI level (CI_β), the NH_2 group is strongly displaced out of plane. The third S_0/S_1 CI located at 3.20 eV is characterized by a strong oop displacement of the O6 atom (CI_γ)[15]. Similar structures were found at different levels of theory[12–14]. The same CIs with very similar structures were also found in aqueous solution[9]. The CI_α^{hyd} is characterized by a pronounced C2-N3 bond length elongation by 0.4 Å, CI_β^{hyd} by an oop displacement of the NH_2 group by $80°$ and CI_γ^{hyd} by an oop displacement of the carbonyl oxygen by $\sim 90°$. In aqueous solution OM2/MRCI locates both CI_β^{hyd} and CI_γ^{hyd} at ~ 3.5 eV. No value for CI_α^{hyd} could be provided.

Surface hopping dynamics simulations in the gas phase showed that relaxation proceeds mainly via CI_α and CI_β. Lan et al. have found 60% of the excited-state population to electronically relax at CI_α (190 fs lifetime) and 40% at CI_β (400 fs lifetime)[15]. Barbatti et al. have found also CI_γ contributing to the excited-state decay: 5% of the excited-state population follows this relaxation path, while 67% undergo internal conversion at a CI associated with a pronounced ring deformation and 28% at a CI associated with an oop displacement of the amino group, similar to CI_β[16].

The situation is significantly different in aqueous solution: Heggen et al.[9] have shown that the relaxation path connecting the FC region with CI_γ^{hyd} becomes the most important one associated with a lifetime of 265 fs or 216 fs for dynamics starting on S_1 or S_2, respectively. In contrast, internal conversion through CI_α^{hyd} and CI_β^{hyd} becomes suppressed. Hopping times associated with those CIs are 343 fs (395 fs) and 441 fs (517 fs) for excitation of S_1 (S_2), respectively. If S_2, i. e. L_b, is excited, internal conversion to S_1 takes on average 21 fs. Due to the dominant relaxation at CI_γ^{hyd}, the average excited-state lifetime of Gua is slightly shorter in solution than in the gas phase[9]. In solution, the excited-state potential energy surface along the path toward the conical intersection exhibits a very steep gradient in the FC region, followed by a flat plateau. In these potential energy regions, the molecule possesses an almost planar purine ring structure. The flat plateau is connected to the conical intersection by a barrierless pathway. Along this reaction path, the molecule loses its planarity[4].

Due to the non-volatility and the low solubility of Gua, there are only very few experimental studies on Gua both in the gas phase and in solution. For isolated Gua molecules, the time-dependent photoion signal was measured by two groups. Kang et al. found a mono-exponential decay with a lifetime of 0.8 ps[2] and Canuel et al. found a bi-exponential excited-state decay with lifetimes of 150 fs and 360 fs[3]. The longer lifetime was corrected to 2.3 ps in a later work of the same group[17]. The situation of Gua is complicated as isolated Gua can exist in different rotameric and tautomeric forms at room temperature. The biologically relevant form is 9H-1H-amino-oxo guanine (1,9H Gua) as shown in Fig. 1. In the gas phase, only about 32% of the Gua molecules are of this canonical form. Overall, there are four different tautomers with abundances $> 1\%$ in the gas phase[18]. The above-mentioned experiments were not tautomer-selective and therefore, the lifetimes correspond to the mixture of excited-state relaxation of different tautomers. There are also two very recent studies on Guo[19] and deprotonated $dGMP^-$[1]. Also here, several tautomers are present. In $dGMP^-$ two contributions were found with lifetimes of 50 fs and 600 fs, respectively. Both lifetimes are assigned to dynamics on the initially excited $S_1(\pi\pi^*)$ state. The fast timescale is due to wave packet motion away from the FC region and the second contribution is then assigned to internal conversion. De Camillis et al. measured the time-resolved photoion yield and focused on the different dynamics of nucleosides compared to isolated DNA bases[19]. They found biexponential behaviour with the faster timescale being in agreement with previous measurements on DNA bases[3]. Interestingly, the longer lifetime was found to be a factor of 2 smaller in the nucleosides than in the corresponding DNA bases for adenosine, thymidine and cytidine. This was explained by an additional relaxation path in the nucleosides opened by a proton transfer through a sugar to base hydrogen bond. Unfortunately, the data on Guo suffered from high noise and the existence of several tautomers and rotamers and the retrieved lifetimes for this molecule did not follow the general trend of the other nucleosides. Instead, lifetimes of 230 fs and 2.3 ps were found, which are both in agreement with lifetimes reported for isolated Gua[3,17]. Hydration strongly affects the tautomeric distributions of Gua and Guo. In aqueous solution of Guo, only one considerably abundant tautomer, the canonical 1,9H Guo form, is found[20]. The presence of the sugar moiety is not expected to influence the energetics or dynamics of the molecule, significantly[21,22].

In the solution phase, the excited-state dynamics of Guo and GMP was investigated by transient absorption and fluorescence up-conversion[4–6,23]. In transient absorption experiments, Karunakaran et al.[4] found three different lifetimes after excitation at 266 nm and 289 nm: 0.2 ps, 0.9 ps and 2.5 ps. At 289 nm excitation is predominantly into S_1, while at 266 nm S_1 and S_2 are excited to approximately equal fractions. S_2, however, is discussed to decay to S_1 much faster than within 100 fs in line with simulations[9]. Also, the motion of the prepared wave packet away from the FC region is discussed to be unresolved, i. e. occuring faster than on a ≈ 100 fs timescale. The fastest lifetime is assigned to the movement of the wave packet between two regions on the potential energy surface, a planar plateau containing a planar pseudominimum and the non-planar minimum. The 0.9 ps lifetime is assigned to internal conversion between the non-planar minimum of S_1 and S_0, while the long lifetime has been ascribed to vibrational cooling of the ground state[4].

Miannay et al. investigated the time-dependent fluorescence upon excitation at 266 nm and found complex dynamics with significant emission wavelength dependence. A global fit revealed also three different lifetimes of 0.16 ps, 0.67 ps and 2.0 ps [6]. These lifetimes are assigned to complex non-exponential dynamics on the S_1 potential energy surface, i. e. the longest observed lifetime is not due to vibrational cooling of the ground state. The strong emission wavelength dependence of the fluorescence dynamics was very surprising and has not been observed in any other DNA base, before [6].

2 Experimental

A 1 mM aqueous solution of Guo, buffered at pH 8 (1 mM tris(hydroxymethyl)-aminomethane (TRIS) and hydrochloric acid (HCl)) is investigated in a liquid jet of about 10 μm diameter. At this pH value, Guo is neutral and the canonical form is the only significantly abundant tautomer present in solution. 30 mM sodium chloride (NaCl) is added to prevent electrokinetic charging of the liquid jet [24]. The experimental setup has been described in great detail elsewhere [25]. Briefly, a regeneratively amplified Ti:Sa laser system delivers 40 fs pulses at 800 nm. One part of the laser output is used to generate 266 nm (4.66 eV) pulses by sum frequency generation in BBO crystals. The remaining part of the laser output is used to pump an optical parametric amplifier (TOPAS, Light Conversion) which delivers pulses between 238 and 248 nm (5.21 and 5.00 eV, respectively). The UV pulses are attenuated to 80-95 nJ for the pump-probe experiment. Guo absorbs strongly at all wavelengths used in the experiment. While at 266 nm, both states, L_a and L_b are excited to about the same extent, at 238 nm-248 nm we excite mainly into the L_b band [4]. However, our temporal resolution (200 fs cross-correlation width) is not sufficient to observe the sub-100 fs transition from L_b to L_a. Hence, the observed dynamics should be dominated by the relaxation on the L_a surface. Due to the ability to excite the molecule at both, the pump and probe wavelength, we expect to observe dynamics in both temporal directions.

The pulses are focused onto the liquid jet to focal spot sizes of about 100 μm. A chopper in each beam allows us to measure the one-color multi-photon signals separately (pump-only and probe-only) and subtract them from the two-color signal on a pulse-to-pulse basis.

Photoelectrons are collected and analyzed by a magnetic-bottle type time-of-flight spectrometer.
Guo and TRIS were purchased from Sigma-Aldrich Co. and sodium chloride from Merck. All substances were used without further purification. The sample solution was prepared using demineralized water (residual conductivity 0.25 μS/cm). At the given pulse intensities, sodium chloride does not contribute significantly to the photoelectron spectra [7].

3 Computational

Starting from the trajectories described in ref. [9] we evaluated the time evolution of the ionization potential of 9H-Gua in water after excitation of the lowest excited singlet state (S_1). As in our former dynamics study, we used the semi-empirical OM2/MRCI method [26,27] as implemented in MNDO99 [28]. Details regarding

the computational method are given in ref. [9]. The present calculation of the ionization potential is based on Koopmans' theorem, i.e. neglecting orbital relaxation and correlation effects (see Supporting Information for details and justification). We performed restricted open-shell OM2-SCF calculations for the lowest open-shell singlet state (S_1) of 9H-Gua in water (two singly occupied orbitals). The first ionization potential was determined from the energy of the highest singly occupied orbital (with appropriate two-electron corrections). In total, 130 trajectories from our previous dynamics investigations were suitable for detailed analysis of the ionization potential. In time steps of 10 fs, single-point calculations were performed for each trajectory and the ionization potential was computed as indicated above. As the ionization potential of the S_1 state is relevant for comparison with experiment, no further single-point calculations were done when the system had hopped to the ground state. Therefore the number of trajectories considered for the computation of the ionization potential declines with time. In the previous study, two different setups were chosen to start the excited-state decay dynamics: The system was either directly excited to the first excited state or to the second excited state (which then very quickly decays to the first excited state). 47 (83) trajectories correspond to the former (latter) case.

As we will show in the results section, our data show evidence for a non-vertical probe transition. To estimate the accessibility of doubly-excited electronic states in Gua we carried out CASSCF calculations on representative geometries obtained from surface hopping dynamic simulations of Gua in aqueous solution [9] followed by the MRCI procedure. For these estimates, the solvent molecules were omitted. We used the aug-cc-pVTZ basis set. In principle, an accurate description of doubly excited states embedded in the ionization continuum, is not possible, because they are coupled to the neighboring ionized states - leading to a decay of the former. As we will not attempt to determine the lifetime of the autoionizing states, we artificially reduce the active space of the CASSCF calculations to avoid the penetration of ionized states. Thus, the active space of the state-averaged CASSCF treatment consists of the HOMO, LUMO and LUMO+1 orbitals (two electrons in three orbitals) ensuring that the four lowest states were S_0, S_1, S_2 and the lowest doubly excited state. We have also tested the inclusion of the HOMO-1 orbital into the active space, but in this very expensive treatment the results did not change, remarkably. Further test calculations show that the next higher doubly excited state is energetically too high to be reached by a one-photon probe step. Consequently, we can restrict ourselves to the lowest doubly excited state.

4 Results

In Figure 2A-C(colormap), the measured time-resolved photoelectron spectra of Guo are shown for different pump and probe wavelengths. At positive delay times the molecule is excited by 266 nm pulses (4.66 eV) and the probe wavelength is 248 nm (A, 5.0 eV), 243 nm (B, 5.1 eV) or 238 nm (C, 5.2 eV). For negative delays, the pulse sequence is opposed. At first glance, the plots look quite indifferent: in all cases, we observe a broad photoelectron distribution at time zero peaking at about 0.7 eV and cover-

ing the full energy range between 0 and 2.5 eV. With increasing delays, this broad distribution seems to shift toward about 0.5 eV and becomes more narrow. At longer delays, also negative pump probe signal is observed which we assign to dead time effects of the MCP detector. Very surprisingly, photoelectron distributions at negative delays nearly mirror those at positive delays (see Fig. S1[29]). This is in contradiction to expecting a shift of the photoelectron distributions toward lower kinetic energies according to the probe photon energy difference. A similar behaviour as in Guo has not been observed in any other system we have studied so far and deserves a detailed discussion subsequent to the description of the experimental and theoretical results.

Following previous experimental observations of Guo in aqueous solution[4,6], we performed a global analysis of the time-dependent photoelectron spectra, assuming a sequential population of different regions on the S_1 surface followed by internal conversion to the ground state. This model involves two rate constants. However, we want to stress that we do not have certain defined states in mind but rather use this bi-exponential description to model a continuous evolution of the wave packet on S_1. We did not consider dynamics on S_2 because we expect this higher excited state to decay to S_1 within our temporal resolution. Therefore, the dynamics of two populations in either delay direction are considered: one is exponentially decreasing at rate k_1, the other one exponentially growing at rate k_1 and decaying at rate k_2. We have introduced a factor γ in the rate equation accounting for structure-dependent ionization cross-sections, i. e. different probabilities to ionize the excited molecule in the two different regions of the S_1 surface. On the other hand, the factor γ may also account for a branching of the relaxation path, i. e. one part of the excited population returns to the ground state with a rate k_1 while the remaining part of the population persists longer in the excited state. This might be the case, if, depending on the initial geometries, only part of the wave packet gets close to the conical intersection at first instance, while the trajectories of the remaining part are more extended until they also encounter the conical intersection. The rate equations and their solution is given in the supporting information[29]. The cross-correlation width (200 fs fwhm) and the temporal origin t_0 were independently determined from nonresonant two-color photoelectron signal of gaseous nitric oxide (NO) and buffer solution. The amplitudes of the two exponentials for every kinetic energy determine the decay-associated spectra (DAS). Details on the fitting procedure are given in the SI[29].

The resulting fit is shown as contour lines on top of the data in Figure 2A-C. The corresponding residuals of these fits are shown in Figure 2D-F(colormap). For comparison, the fit contour lines are displayed on top of the residuals, too. The model fits the data very well, no systematic residuals are apparent. Nevertheless, we note that the data can be equally well fitted by assuming a model with a parallel relaxation path. The population dynamics (G-I) and DAS (J-L) retrieved from the global fit are displayed as well.

The fit results are summarized in table 1. For dynamics in positive delay direction, we find a shorter lifetime of about 290 fs and a longer one of about 2.3 ps. In negative delay direction, faster dynamics are observed: the shorter lifetime is about 50 fs, the longer one is about 1.1 ps.

For all pump and probe wavelength combinations, we find $\gamma \approx$ 0.3. As already discussed before, this might be due to structure-dependent ionization cross section, i. e. ionization of the excited molecule is initially about 3 times more likely than at later times. On the other hand, it may also indicate that there is a branching in the relaxation path and 70% of the population decays to the ground state with rate k_1 and only 30% remain in the excited state for longer. From the comparison of signal at negative and positive delay times, conclusions on the wavelength dependent ionization cross-sections are possible. The signal ratio is given by

$$\frac{A_+}{A_-} = \frac{\alpha_{GS}(4.66\,\text{eV})}{\alpha_{GS}(5.0-5.2\,\text{eV})}\frac{\alpha_{ES}(5.0-5.2,\text{eV})}{\alpha_{ES}(4.66\,\text{eV})}, \quad (1)$$

where α_{GS} is the absorption coefficient of the ground state molecule and α_{ES} is the absorption coefficient of the excited molecule. The ground state absorption of Guo is well known[30]. We have evaluated only the signal associated with the slower decay because this is less sensitive to the particular fit parameters. For the individual photon energy combinations we find A_+/A_- to be 0.46 (4.66 eV / 5.0 eV), 0.7 (4.66 eV / 5.1 eV) and 1.04 (4.66 eV / 5.2 eV) and deduce excited-state absorption coefficient ratios $\alpha_{ES}(4.66\,\text{eV})/\alpha_{ES}(5.0-5.2\,\text{eV})$ of 1.7 (5.0 eV) and 1.3 (5.1-5.2 eV).

The DAS are presented in Fig. 2 J-L. In addition, we compare the normalized DAS obtained for the different pulse sequences at different wavelength combinations in the supporting information Fig. S1. As already evident from the data we find also the DAS to be nearly independent of the pulse sequence. Any differences between the spectra associated with a given decay obtained with a given photon energy combination are much smaller than the probe photon energy difference, i. e. 0.34 eV-0.54 eV. There are some differences for the spectra associated with the fast decay which we mainly assign to limits of the global fitting and inaccuracy of the independent determination of cross-correlation width and temporal overlap.

Fig. 3 shows the time-dependent ionization energies calculated from Koopmans' theorem averaged over all different trajectories for Gua. No significant difference was observed for different groups of trajectories (as characterized by the respective hopping geometries). We observe that the average ionization potential of the S_1 state quickly rises from an initial value of about 3-4 eV to a value in the range of 5-6 eV, typically within 50 fs. We attribute this to fast initial dynamics in the S_1 state, with concomitant stabilization. An association with the steep gradient of the S_1 surface in the FC region seems obvious. At $t = 0$, we find a S_1 ionization energy of 3.54 eV which can be used for calibration against experimental data. With an applied shift of -1 eV we find very good agreement with our experimental data (cf. Fig. 3b).

Besides the time-dependent ionization energies we also retrieve the time-dependent population of the S_1 state from our calculations, which is also shown in Fig. 3a. The computed lifetime is 314 fs for Gua which is significantly shorter than the experimentally observed ps lifetime for Guo. In a previous work, these deviations were suggested to be due to the different substituents at the N9 position[9].

Table 1 Retrieved timescales for the excited-state relaxation of aqueous Guo obtained for different pump and probe photon energies. Additionally, the relative intensity γ of the fast and slow contributions is given. Provided uncertainties are retrieved from the χ^2 fitting procedure. †This lifetime was kept constant.

	pump / eV	probe / eV	τ_{fast} / fs	τ_{slow} / ps	$\gamma = A_{slow}/A_{fast}$
positive delays	4.66	5.00	380±40	2.4±0.3	0.32
	4.66	5.10	260±60	2.3±0.4	0.34
	4.66	5.21	250±20	2.1±0.1	0.42
negative delays	5.00	4.66	40±10	1.1±0.1	0.24
	5.10	4.66	60±30	1.1†	0.34
	5.21	4.66	60±10	1.0±0.1	0.29
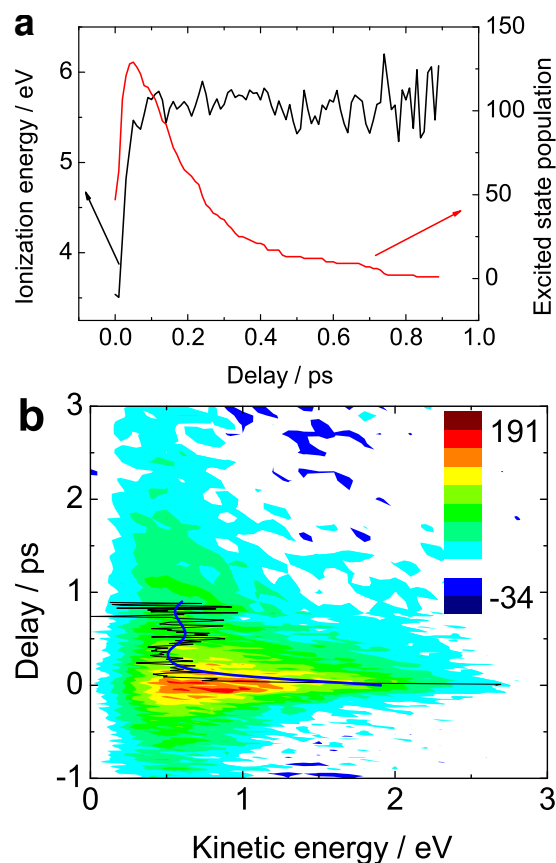
Fig. 3 a) Time-dependent ionization energy of the S_1 state calculated from Koopmans' theorem (black) and S_1 state population (red). b) Comparison between computational and experimental results (4.66 eV+5.2 eV). Computational results (black) were shifted by -1.0 eV to match the experimental values (contour plot). To account for the limited time resolution, the time-dependent calculated ionization energies were convolved with a Gaussian of 200 fs FWHM (blue).

5 Discussion

In the following we suggest two alternative interpretations of the observed dynamics. One follows the interpretation of recent experimental work on aqueous Guo or GMP[4,6]: The first component is ascribed to the wave packet in the FC region that quickly relaxes due to initial dynamics on the S_1 surface concomitant with a fast rise of ionization energy. The second component is assigned to the wave packet evolving from the flat plateau to the conical intersection. In this region, no significant dependence of the ionization energy on the reaction coordinate (or time) is observed.

We assign the decay of this component to the internal conversion to the ground state at the conical intersection. The S_1 lifetime is therefore $\sim 2.1 - 2.4$ ps for excitation at 4.66 eV and 1.0-1.1 ps for excitation at 5.2 eV.

However, our finding that only 30% of the initially excited population is observed in the longer-lived signal allows also an alternative interpretation. As already indicated before, it is conceivable that (depending on the initial geometries) only a part of the wave packet (70%) quickly encounters the conical intersection (with rate $k_1 = (290 fs)^{-1}$), while the remaining part is too far away in phase space and needs more time to explore the potential energy surface and to find the conical intersection (rate $k_2 \sim (2.3 ps)^{-1}$). Further indirect support comes from the recent work of De Camillis et al.[19] in conjunction with our simulation. They have found significantly faster dynamics in the nucleosides with respect to the bases for adenine, thymine and cytosine. Their guanine results however suffered from more noisy data and the presence of different tautomers in the gas phase. If we nevertheless presume a general mechanism for all DNA bases, i. e. a charge-transfer state opening a new relaxation route, the dynamics should be faster (not slower) in Guo than in Gua. Therefore the simulation results should represent an upper limit for the excited state lifetime of Guo. Indeed, the observed lifetime in the simulation of 314 fs is in very good agreement with rate k_1.

It is interesting to compare the observed dynamics in water with those of isolated molecules. De Camillis et al. have retrieved lifetimes which are in very good agreement with our results, both for the fast and slow component, indicating that the solvent environment does not have a huge influence in this case and dynamics is governed by internal degrees of freedom[19]. However the error bars are quite large and the sample was a tautomeric and rotameric mixture in their work. For this reason, a direct comparison of the two different experiments is difficult. Chatterley et al. have performed similar experiments as we did on isolated dGMP$^-$, i. e. they measured photoelectron spectra. They observed somewhat faster dynamics (50 fs/600 fs) than we did (290 fs/2300 fs), but the interpretation is very similar to the first interpretation that we suggested: The fast timescale is due to wave packet motion away from the FC region, while the second component is due to internal conversion. This assignment was motivated by the similarity of timescales as observed for hydrated dGMP$^-$. Nevertheless, a branching of the trajectories can likewise explain the observations.

In the following we will further discuss our data in the frame of the first interpretation provided for the observed dynamics (no

branching). We emphasize, however, that the second interpretation would lead to the same conclusions. We will now turn the discussion to the nearly identical decay associated spectra for the different pulse sequences. As discussed in the literature [4,9], we expect to observe dynamics in the S_1 state for either pump pulse. For vertical ionization we do expect to observe photoelectron kinetic energy distributions that reflect the differences in probe photon energy. This is apparently not the case here. Assuming, that the ionization cross section does not depend on the probe photon energy in a very peculiar way, the results suggest that either dynamics is observed in different states (i. e. S_1 and S_2) or the transition in the probe step is not vertical for at least one of the two pulse sequences. There is no reason to question the interpretation from previous experiments and simulations that there is an ultrafast population transfer from S_2 to S_1 within a few tens of fs. Therefore, we have to refuse that the probe photon absorption is accompanied by a vertical transition to the ionic state. We suggest the existence of a metastable electronic state, embedded in the ionization continuum. According to our hypothesis, the same vibronic levels of this electronic state are populated, irrespective of the sequence of the two light pulses. We suppose that this metastable state is a doubly excited one, characterized by a simultaneous excitation of two valence electrons, $(\pi^*)^2$, decaying vertically to the ionic ground state D_0, where the kinetic energy of the ejected photoelectrons is given by the difference of the doubly-excited-state potential energy and the ground-state ion potential energy.

These two situations, ionization via a doubly-excited state and direct ionization are sketched in Fig. 4. The pump pulse of a given photon energy prepares the molecule in the electronically excited S_1 state with a certain amount of kinetic energy stored in different vibrational modes. This excess energy can be distributed among further vibrational modes via intramolecular vibrational redistribution (IVR) or released to the solvent via intermolecular energy transfer (IET). There is not much known about the vibrational cooling dynamics in the excited S_1 state of neutral Guo, because it is superimposed by the very fast internal conversion to the ground state. However, in protonated GMP vibrational cooling dynamics in S_1 takes about 3 ps [31]. We can assume, that this dynamics is similar in the neutral molecule, i. e. slower than internal conversion and that there is no significant redistribution of excess vibrational energy in the course of excited-state relaxation. Transition to the doubly-excited state cannot be vertical for both pulse sequences. The vibrational energy distribution of the molecule in the doubly-excited state is not necessarily the same as for the molecule in the S_1 state. If the doubly-excited state was not involved, the photoinduced transition to the ionic ground state would be vertical and the vibrational energy distribution of the molecule in the S_1 state would remain in the ion. The photoelectron kinetic energy is then the difference of absorbed probe photon energy and the potential energy difference between the S_1 and D_0 state. On the basis of a simple model (one- and three-dimensional harmonic oscillator), the behaviour of the photoelectron spectrum is compared for auto- and direct ionization in the SI [29]. Our ab-initio calculations show that, except for $t = 0$, in all investigated geometries the lowest doubly

excited state is located in an accessible energy range above S_1 and is nearly parallel to it (deviations not larger than 0.5 eV). Investigating the electron configuration of this doubly excited state, we found that for all geometries the predominant contribution ($> 95\%$) is of $(\pi^*)^2$ character. In the SI [29], this orbital is shown and compared with the HOMO. The transition dipole moment for the excitation of the doubly excited state from S_1 is comparable to or even larger than that of the S_0–S_1 transition. This means that, in principle, the cross section for excitation of the 2xEx state is sufficiently high. Of course, in a more detailed probe absorption treatment, interference effects between discrete and continuum states have to be considered, leading to Fano spectral features [32]. Such fingerprints of the doubly excited state were not observed in our experiments, presumably, because of the remarkable spectral broadening due to vibronic substructure and the water environment. In most cases the doubly-excited state is energetically located $\sim 0.5 - 1.5$ eV above the ionization limit, i. e. explaining the observed photoelectron kinetic energies. Detailed results of the calculations are provided in the supporting information [29].

If ionization occurs via the doubly-excited state as we suggest, the observed kinetic energies are given by the difference between the doubly-excited and the ionic state. The binding energy of the initially excited S_1 state is generally not reflected in the data. So, the question arises, why the calculated S_1 ionization energies are fitting the data so nicely. From our calculations we suggest that the doubly-excited-state potential energy depends similarly on the reaction coordinate as the S_1 state, i. e. the S_1 binding energy differs from the difference of doubly-excited and ionic potential only by a nearly constant value.

While the kinetic energy distribution may not contain direct information about the S_1 potential energy surface, the time-dependent photoelectron signal clearly reflects excited-state population dynamics together with structure dependent excited-state absorption cross-sections. We found faster dynamics when the molecule was excited at 5.0-5.2 eV than at 4.66 eV. This can be discussed in different ways:

a) Accelerated dynamics due to higher excess energy. Excitation at higher photon energies prepares the excited state with higher vibrational energy. This generally leads to faster dynamics. For pump wavelengths of 266 nm and 287 nm, however, no significant difference in the dynamics was observed [4]. Nevertheless, the situation may be different at 238 nm, which is also indicated by surface hopping dynamics simulations. They yielded slightly faster excited-state decays after initial excitation of S_2 than of S_1 [9].

b) Faster dynamics due to accessibility of additional relaxation pathways. Due to the higher excess energies in the excited state, new relaxation pathways may open [6].

c) Limited FC windows for ionization. At negative delays the excited state is probed with 4.66 eV photons, i. e. at lower energy than at positive delays. If the energy gap between excited and ionic state increases above the probe photon energy, the excited state becomes invisible for the probe pulse in photoelectron spectroscopy. This point is reached faster for a smaller probe photon energy, i. e. the observed dynamics seem to be faster.

In the presence of the doubly-excited state, point c is not relevant, because the accessibility of the final state is only given by the total absorbed photon energy.

Our retrieved timescales compare well with timescales found in transient absorption and fluorescence up-conversion[4,6]. However, in contrast to fluorescence up-conversion and transient absorption we only need two components to satisfactorily describe our data. We want to stress that we do not intend to assign these two lifetimes to defined states on the S_1 potential energy surface but rather use them to describe a continuous evolution of the excited wave packet. We also want to note that in agreement with fluorescence up-conversion our data suggest that the longest observed timescale is due to dynamics in the S_1 state, most likely related to S_1 population decay due to internal conversion, and does not reflect ground state cooling.

It is interesting to investigate the DAS in more detail. At first glance it is striking, that the photoelectron spectrum is initially very broad (FWHM of the first component is ~ 1.5 eV) and becomes significantly more narrow at later times (FWHM of the second component is ~ 1.0 eV). This may at first be surprising since the wave packet is expected to spread out on the flat S_1 surface which could be expected to transfer into very broad photoelectron spectra. However, we will show that the particular potential energy landscape for Guo/Gua readily explains this observation. The wave packet in S_1 is prepared by the pump pulse where the vibrational ground state wavefunction is projected onto S_1. In the FC region, the S_1 potential energy surface possesses a very steep gradient and we suggest that this is also the case for the doubly-excited state. I. e. in this region, ionization energies of S_1 as calculated from Koopmans' theorem and potential energy differences between the doubly-excited and the ionic ground state have very different values. This transfers into a very broad distribution of resulting photoelectron kinetic energies. This very steep potential gradient in the FC region of the S_1 state leads to a very fast stabilization of the excited state within about 290 fs (in case of 4.66 eV excitation). This is sketched in Fig 5. On the other hand, our calculations show, that after this initial stabilization the ionic potential along the reaction coordinate is parallel to the S_1 and the doubly-excited-state potential. Therefore, even a strongly broadened wave packet will lead to a narrow photoelectron band. The observed width of ~ 1 eV is typical for hydrated species and mainly caused by inhomogeneous broadening due to very different local solvation structures[33,34].

6 Conclusion

We have investigated the excited-state relaxation in aqueous Guo by time-resolved photoelectron spectroscopy. Dynamics were initiated by pulses at 266 nm, 248 nm, 244 nm or 238 nm on the S_1 or S_2 potential energy surface. The $S_2 \longrightarrow S_1$ transition was not resolved in our experiments and the data therefore reflects dynamics in the S_1 state. In agreement with our surface hopping dynamic simulations, the photoelectron spectrum rapidly shifts towards smaller kinetic energies until it stabilizes at a kinetic energy of about 0.5 eV. The spectrum also narrows significantly. We have suggested two alternative interpretations of the observed
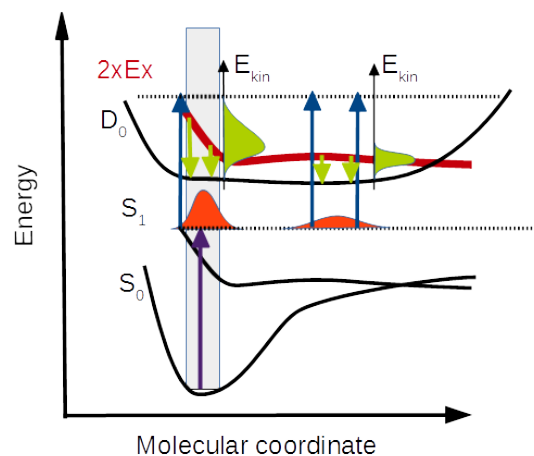
Fig. 5 Schematic potential energy curves of Guo in water. The pump pulse launches an excited-state wave packet (orange) in the Franck-Condon region (grey) of the populated S_1 or S_2 (not shown) state. The S_2 state decays within the time resolution into S_1. The time-dependent S_1 ionization energy (along the relaxation path) is nearly constant besides a sharp initial rise, leading to the sketched ionic potential curve D_0. Around the temporal overlap of both pulses, the steep gradient of the excited state in the FC region is mapped into a very broad photoelectron kinetic energy distribution (light green). With increasing delays, the wave packet dephases and spreads on the excited-state potential. Ionization in the flat region of the S_1 potential leads to a more narrow distribution of photoelectrons due to the parallelity of the doubly-excited 2xEx state and D_0.

dynamics. The first one follows the interpretation of recent experimental results of hydrated Guo and GMP[4,6]. The fast shift is assigned to initial dynamics in the S_1 state: relaxation from the steep FC region to the rather flat plateau occurs in about 290 fs if dynamics are initiated by 266 nm pulses. This is followed by a slower signal decay within ~ 2.3 ps which we assign to internal conversion at a conical intersection. We have observed that only 30% of the initially excited population contributes to the signal of the slower decaying component. This might be due to structure-dependent ionization cross section. On the other hand, this finding can also suggest an alternative interpretation: The dominant part (70%) of the initially excited population encounters the conical intersection with the ground state very fast and gives rise for the observed decay rate $k_1 = (290 \text{fs})^{-1}$ in agreement with the S_1 lifetime observed in our simulation, while the remaining part of the initially excited population (30%) follows more extended trajectories in phase space and needs more time to encounter the conical intersection. This part of the population gives rise to the observed second decay rate $k_2 = (2.3 \text{ps})^{-1}$. More investigations are needed to decide in favor of one or the other relaxation model. Time-resolved photoelectron imaging experiments allowing to also measure the angular distribution of the photoelectrons may be one promising technique to solve this problem[35]. As it was shown theoretically for NO_2[36] such measurements may allow to obtain a clearer picture of ionization channels near a conical intersection. However, it is currently not possible to apply this technique to highly volatile samples.

Interestingly, our photoelectron kinetic energy distributions

show that the probe step is not vertical, i. e. the measured photoelectron kinetic energy distributions do not depend on the probe photon energy in the range applied here. We suggest that this is due to population of a doubly-excited state in the probe step which rapidly decays via autoionization. These results show that in time-resolved photoelectron spectroscopy the photoelectron kinetic energy distributions can be dominated by intermediate transients even in a one-photon probe step and that the analysis and discussion of such data requires great care. In diatomic molecules, doubly-excited autoionizing states have been investigated and studied in some detail [37,38]. To the best of our knowledge this is not the case for larger molecules.

7 Acknowlegdgements

References

1 A. S. Chatterley, C. W. West, V. G. Stavros and J. R. R. Verlet, *Chem. Sci.*, 2014, **5**, 3963.

2 H. Kang, K. T. Lee, B. Jung, Y. J. Ko and S. K. Kim, *Journal of the American Chemical Society*, 2002, **124**, 12958–12959.

3 C. Canuel, M. Mons, F. Piuzzi, B. Tardivel, I. Dimicoli and M. Elhanine, *J. Chem. Phys.*, 2005, **122**, 074316.

4 V. Karunakaran, K. Kleinermanns, R. Improta and S. A. Kovalenko, *J. Am. Chem. Soc.*, 2009, **131**, 5839–5850.

5 J. Peon and A. H. Zewail, *Chem. Phys. Lett.*, 2001, **348**, 255–262.

6 F.-A. Miannay, T. Gustavsson, A. Banyasz and D. Markovitsi, *J. Phys. Chem. A*, 2010, **114**, 3256.

7 F. Buchner, H.-H. Ritze, J. Lahl and A. Lübcke, *Phys. Chem. Chem. Phys.*, 2013, **15**, 11402.

8 F. Buchner, A. Nakayama, S. Yamazaki, H.-H. Ritze and A. Lübcke, *J. Am. Chem. Soc.*, 2015, **137**, 2931.

9 B. Heggen, Z. Lan and W. Thiel, *Phys. Chem. Chem. Phys.*, 2012, **14**, 8137.

10 R. Improta and V. Barone, *Topics in Current Chemistry*, Springer Berlin Heidelberg, 2014, pp. 1–29.

11 M. Parac, M. Doerr, C. M. Marian and W. Thiel, *J. Comput. Chem.*, 2010, **31**, 90.

12 H. Chen and S. Li, *J. Chem. Phys.*, 2006, **124**, 154315.

13 C. M. Marian, *J. Phys. Chem. A*, 2007, **111**, 1545.

14 L. Serrano-Andres, M. Merchan and A. C. Borin, *J. Am. Chem. Soc.*, 2008, **130**, 2473.

15 Z. Lan, E. Fabiano and W. Thiel, *ChemPhysChem*, 2009, **10**, 1225.

16 M. Barbatti, J. J. Szymczak, A. J. A. Aquino, D. Nachtigallova and H. Lischka, *J. Chem. Phys.*, 2011, **134**, 014304.

17 M. Mons, I. Dimicoli and F. Piuzzi, in *Isolated Guanine: Tautomerism, Spectroscopy and Excited State Dynamics*, Springer, Dordrecht, London, 2008, ch. pp. 343-367.

18 Y. H. Jang, W. A. G. III, K. T. Noyes, L. C. Sowers, S. Hwang and D. S. Chung, *J. Phys. Chem. B*, 2003, **107**, 344.

19 S. D. Camillis, J. Miles, G. Alexander, O. Ghafur, I. D. Williams, D. Townsend and J. B. Greenwood, *Phys. Chem. Chem. Phys.*, 2015, **17**, 23643.

20 H. T. Miles, F. B. Howard and J. Frazier, *Science*, 1963, **142**, 1458.

21 C. E. Crespo-Hernández, B. Cohen, P. M. Hare and B. Kohler, *Chem. Rev.*, 2004, **104**, 1977.

22 C. T. Middleton, K. de La Harpe, C. Su, Y. K. Law, C. E. Crespo-Hernández and B. Kohler, *Annu. Rev. Phys. Chem.*, 2009, **60**, 217.

23 J.-M. L. Pecourt, J. Peon and B. Kohler, *J. Am. Chem. Soc.*, 2001, **123**, 10370.

24 N. Preissler, F. Buchner, T. Schultz and A. Lübcke, *J. Phys. Chem. B*, 2013, **117**, 2422.

25 F. Buchner, A. Lübcke, N. Heine and T. Schultz, *Rev. Sci. Instr.*, 2010, **81**, 113107.

26 W. Weber and W. Thiel, *Theor. Chem. Acc.*, 2000, **103**, 495.

27 A. Koslowski, M. E. Beck and W. Thiel, *J. Comp. Chem.*, 2003, **24**, 714.

28 W. Thiel, *MNDO program, version 6.1*, 2007, Mülheim.

29 *Supporting information*.

30 D. Voet, W. B. Gratzer, R. A. Cox and P. Doty, *Biopolymers*, 1963, **1**, 193.

31 Y. Zhang, R. Improta and B. Kohler, *Phys. Chem. Chem. Phys.*, 2014, **16**, 1487.

32 U. Fano, *Phys. Rev.*, 1961, **124**, 1866.

33 C. Schroeder, E. Pluhařová, R. Seidel, W. P. Schroeder, M. Faubel, P. Slavíček, B. Winter, P. Jungwirth and S. E. Bradforth, *J. Am. Chem. Soc.*, 2015, **137**, 201.

34 A. Lübcke, F. Buchner, N. Heine, I. V. Hertel and T. Schultz, *Phys. Chem. Chem. Phys.*, 2010, **12**, 14629.

35 P. Trabs, F. Buchner, M. Ghotbi, A. Lübcke, H.-H. Ritze, M. J. J. Vrakking and A. Rouzée, *J. Phys. B.: At. Mol. Opt. Phys.*, 2014, **47**, 124016.

36 Y. Arasaki, K. Takatsuka, K. Wang and V. McKoy, *J. Chem. Phys.*, 2010, **132**, 124307.

37 T. Baumert, M. Grosser, R. Thalweiser and G. Gerber, *Phys. Rev. Lett.*, 1991, **67**, 3753.

38 G. Sansone, F. Kelkensberg, J. F. Pérez-Torres, F. Morales, M. F. Kling, W. Siu, O. Ghafur, P. Johnsson, M. Swoboda, E. Benedetti, F. Ferrari, F. Lépine, J. L. Sanz-Vicario, S. Zherebtsov, I. Znakovskaya, A. L'Hullier, M. Y. Ivanov, M. Nisoli, F. Martín and M. J. J. Vrakking, *Nature*, 2010, **465**, 763.
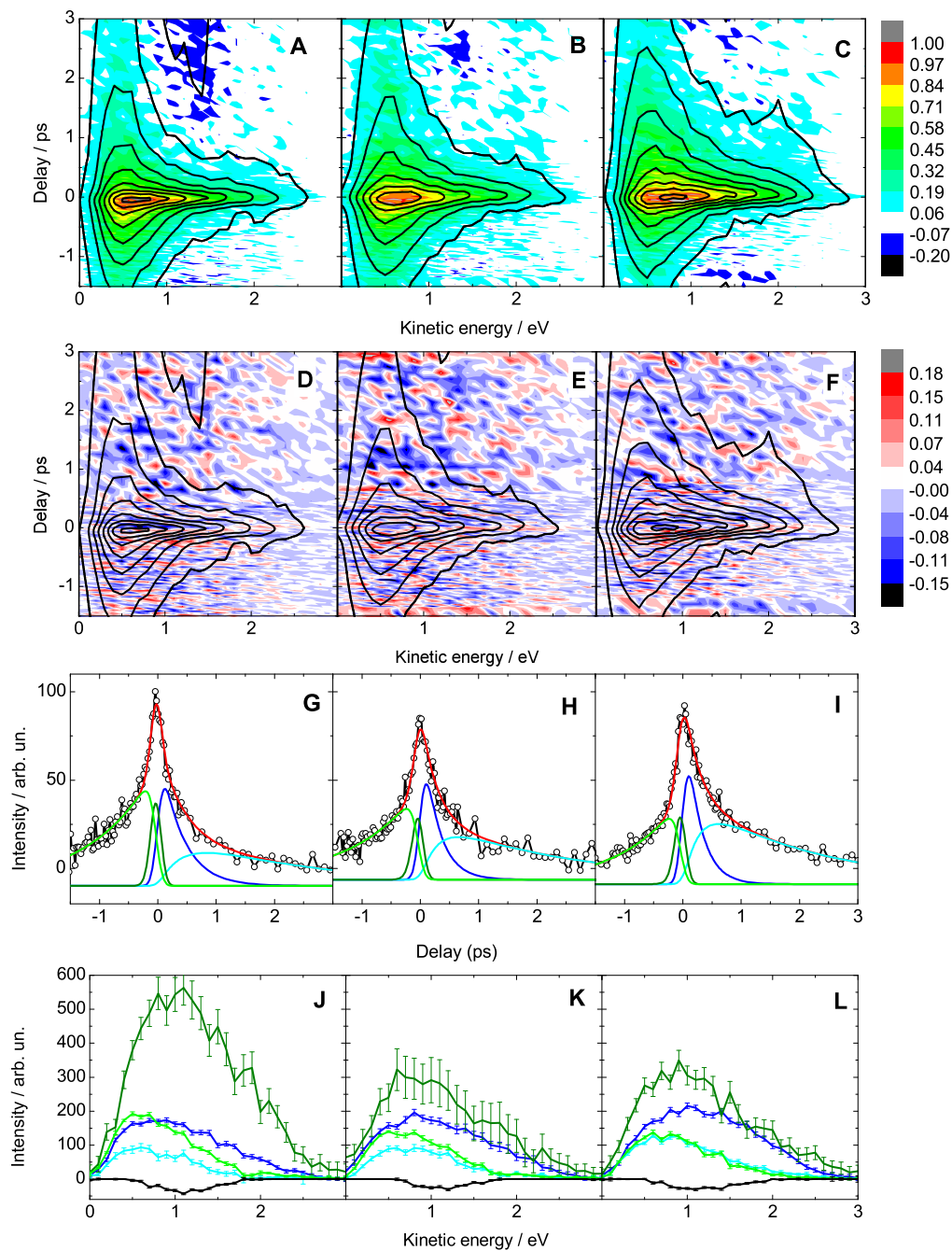
Fig. 2 Time-resolved photoelectron spectra of Guo excited and ionized at different photon energies: A, D, G, J: 4.66 eV+5.0 eV, B, E, H, K: 4.66 eV+5.1 eV, C, F, I, L: 4.66 eV+5.2 eV. A, B, C: raw data (color map) and fit (contour lines); one-color signal has been subtracted. D, E, F: residuals (color map) and fit (contour lines). G, H, I: Population dynamics obtained from the global fit. Dots mark energy-integrated raw data. The red line is the sum of the individual population dynamics. J, K, L: decay-associated spectra (same color code as for the population dynamics). Provided error bars are retrieved from the χ^2 fitting procedure.
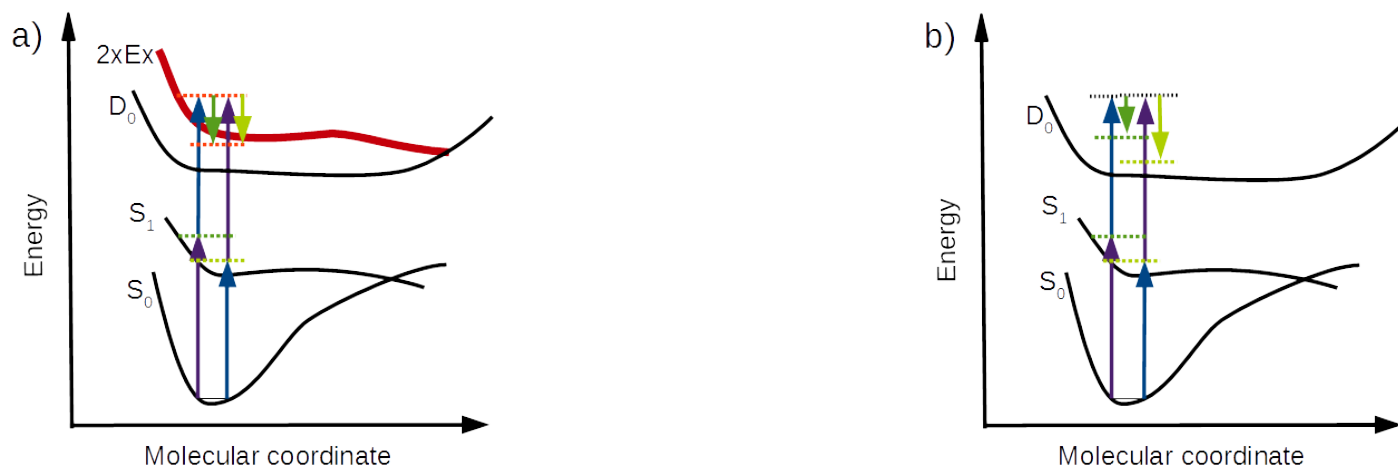
Fig. 4 One-dimensional sketch of potential energy surfaces and the photoionization processes in the presence of a doubly-excited state 2xEx (a) and in its absence (b). Blue and violet arrows represent the two different photon energies. Different green arrows represent photoelectron kinetic energies for the two different pulse sequences.